Tanzania Journal of Science 46(2): 449-459, 2020
ISSN 0856-1761, e-ISSN 2507-7961

Comparison of Experimental and Monte Carlo Simulation of Angular Distributions of Bremsstrahlung Photons from 28-GHZ Electron Cyclotron Resonance (ECR) Ion Source

Mwingereza J. Kumwenda
Nuclear Science Research Group, Department of Physics, University of Dar es Salaam, P. O. Box 35063, Dar es Salaam, Tanzania
E-mail address: kmwingereza@udsm.ac.tz
Received 30 Dec 2019, Revised 28 May 2020, Accepted 6 June 2020, Published June 2020
DOI: https://dx.doi.org/10.4314/tjs.v46i2.21

Abstract
Angular distributions of deceleration radiation or *bremsstrahlung* in German, both experimental and simulated from Electron Cyclotron Resonance Ion Source (ECRIS) are not well understood so far. The *bremsstrahlung* photons of the angular distributions from 28-GHz ECR ion source at Busan Centre of Korea Basic Science Institute (KBSI) were measured in nine azimuthal angles for the first time. Three round type NaI(Tl) detectors were used to measure the angular distributions of the bremsstrahlung photons emitted at the extraction side of the ECRIS at the same time. Another NaI(Tl) detector was placed downstream from the ECR ion source for monitoring photon intensity. The ECR ion source was operated at RF power of 1 kW. Monte Carlo simulation based on Geant4 package was performed to study the angular distributions of the bremsstrahlung photons. The simulation was based on a full geometry of the ECR ion source. Geant4 simulation was executed to take the geometrical acceptance and energy-dependent detection efficiency into account due to large non-uniformity in the material budget. True bremsstrahlung energy spectra from the 28-GHz ECR ion source were obtained using the inverse-matrix deconvolution method. The deconvolution method was based on a full geometry of the Geant4 model of the ECR ion source. It is interesting to observe that the maximum simulated photon yields at angle 150° was correlated with the measured photon yields at angle 150° at the extraction side, which can be explained by the internal structure and shape of the ECR plasma.

Keywords: Angular distribution, *Bremsstrahlung* photons, Deconvolution, ECRIS, Geant4 simulation, NaI(TI) detectors, RF power.

Introduction
Electron cyclotron resonance ion sources (ECRIS) are magnetized plasma ion sources used to produce intense multiply charged ions taking advantage of accelerating electrons in the magnetic field with a GHz range radio frequency microwave. The multiply charged ions are produced inside the plasma and confined by magnetic fields. Due to the unique capability of producing highly charged ion beams, the ECR ion sources have been utilized in heavy ion accelerators, nuclear and atomic physics research (Kasthurirangan et al. 2012, Park et al. 2016).

Modern electron cyclotron resonance (ECR) ion sources, including that found at the Korea Basic Science Institute (KBSI), consist of a mirror field (generated from 3 solenoid coils) combined with hexapole magnetic fields for plasma confinement (Leitner et al. 2006, Park et al. 2016). The reason for combining hexapole fields and mirror field is plasma instabilities which prevent stable plasma confinement caused by simple mirror structure (without hexapole). To prevent the plasma instability, some sort of the field was required that ensures the centre of the plasma sees increasing field strength in all directions was applied. To achieve this, a hexapole field is added to the simple mirror. This leads to a configuration where the plasma is confined by the solenoids and where the plasma instabilities are suppressed by the hexapole field, which is called a min-B configuration (Lieberman and Lichtenberg 2005).

In the ECR ion sources, radio frequency microwaves heat plasma electrons in order to provide ionization of neutral gases. As a result of ECR heating, very high electron energies are produced which can generate a large amount of "deceleration radiation" or *bremsstrahlung* photons (Leitner et al. 2007, Ropponen et al. 2009). Two processes in the ECR plasma lead to the emission of the bremsstrahlung photons in the form of X-rays. First bremsstrahlung is created by electron-ion collisions within the plasma volume. The second process is when electrons are lost from the plasma, collide with the plasma chamber wall and radiate bremsstrahlung due to their sudden deceleration (Noland et al. 2010).

The produced bremsstrahlung photons deposit energy in the structure of ion sources and turn out to be substantial heat load to the cryostat in the case of superconducting ECR ion sources (Leitner et al. 2006, Zhao et al. 2010). The cryogenic system can remove only a limited amount of the heat from the cryostat. If more heat is added to the system than can be removed, the temperature of the liquid helium rises and can cause the superconducting coils to quench (Park et al. 2016).

Bremsstrahlung photons generated inside the ECR ion source have been measured since early 1960s (Noland 2011). Nevertheless, many of the previous experiments used to measure the bremsstrahlung photons in only one direction, axially using one or two detectors but under different conditions. However, the bremsstrahlung photons emitted from the ECR are expected to be anisotropic due to various effects (Noland et al. 2010). Thus, this paper presents the first experimental and simulated results of the angular distributions of the bremsstrahlung photons at the extraction of the ECR ion source at nine and twelve azimuthal angles, respectively. The aim of this study was to compare experimental and Monte Carlo simulation of the angular distribution of the bremsstrahlung photons from 28-GHz ECR ion source and thereafter to unveil the sources of large number of photons events observed at some angles based on the Geant4 simulations and the measurements.

Materials and Methods

Experimental Setup

Experiments were carried out to measure the angular distributions of the bremsstrahlung photons from 28GHz ECR ion source of the compact linear accelerator facility at KBSI, cyclotron research centre. The ECR ion source established at the KBSI is comprised of six racetrack hexapole coils and three mirror solenoid magnets (Park et al. 2014). The axial magnetic field is about 3.6 T at the beam injection area and 2.2 T at the extraction region, respectively. A radial magnetic field of 2.1 T can also be achieved on the plasma chamber wall. The three solenoid magnets were assembled with stainless steel pipe whereas step-type racetrack coils were placed around the aluminium bore tube. The cylindrical plasma chamber is 500 mm long and 150 mm in diameter, respectively (Lee et al. 2012).

The experimental setup to measure the angular distributions of the bremsstrahlung photons in this study differs from previous experiments performed by other scholars (Benitez et al. 2008, Noland et al. 2010). This study used four identical cylindrical NaI(TI) detectors (508 mm by 508 mm); three round type detectors placed at the radial position and one detector at the view port. Photon energy spectra were measured using three round type NaI(TI) detectors as shown in Figure 1 facing the edge of the ECRIS at the extraction side of the ECR ion source. For easy reference, all detectors were labelled with letters D1, D2, D3 and D4, which were operated at +1300 V. The three detectors (D1, D2 and D3) were mounted on the support structure for measurements at azimuthal angles, as shown in Figure 1, while the D4 detector was mounted at the view port for monitoring the intensity of the ECR plasma as depicted in Figure 2 (Kumwenda et al. 2017).

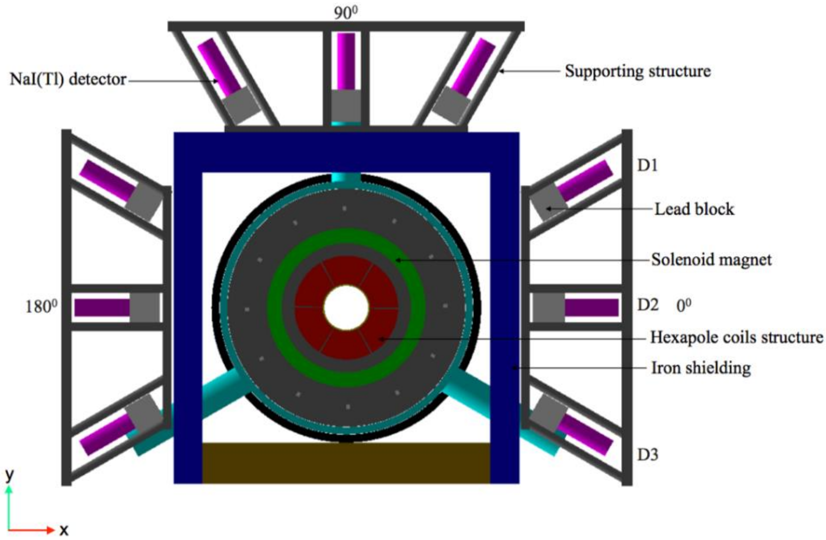

Figure 1: Schematic view of the nine azimuthal angles measured using NaI(Tl) detectors at the extraction side.

At first setup, the three-round type NaI(Tl) detectors coupled to 12-stage photomultipliers were in the configurations of D1, D2, and D3 to the extraction side of the ECR ion source. For systematic study among the three detectors, in the same position the detectors configurations were exchanged for D2, D3, and D1 and lastly the detectors were located in the order of D3, D1, and D2. The detectors were exchanged positions in all nine radial positions in order to cover the angular region. The photon energy was measured at 9 angles in a 30° interval at the extraction side of the ECR ion source. The detectors were placed at the three sides explicitly right, top and left of the iron shielding structure as depicted in Figure 1, the distance between these detectors and the ECRIS iron shielding was about 20 mm (Kumwenda 2018).

To minimize the effects of background radiations, each NaI(Tl) detector was placed in a lead (Pb) collimator of a 0.5 cm hole. The Pb collimator covered a full dimension of the NaI(Tl) crystal. The 500 MHz Flash Analog-to-Digital Converter (FADC) system was used for data acquisition as illustrated in Figure 3. The detectors signal was fed to splitting module and then to a 500-MHz FADC (NKFADC500) and recorded in a coincidence with a reference signal from the detector D4 placed at the view port. The 4-channel flash ADC module (Notice Co.) recorded full pulse information from four NaI(Tl) detectors in every 1 μs. The full pulse shape taken using NaI(TI) detectors are shown in Figure 4. The ring-buffer data were then fed to a PC. Trigger logic OR provided event triggering conditions. The data recorded by using the NKFADC500 flash ADC were in raw binary form. The raw binary data were decoded to get ROOT format data for analysis (Kumwenda 2018).

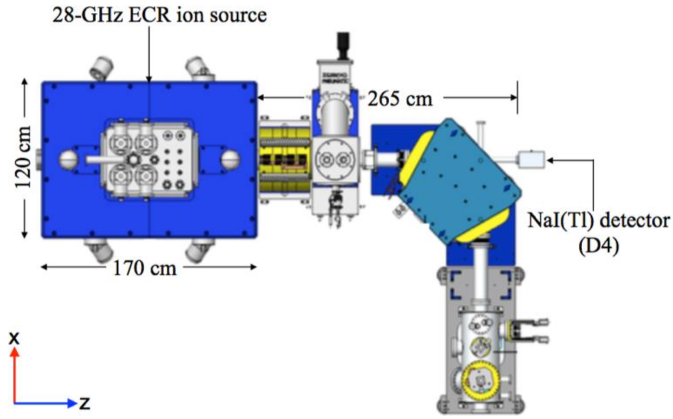

Figure 2: Fourth detector (D4) at the view port of the ECR ion source used to monitor a possible variation in ECR plasma intensities throughout the measurements.

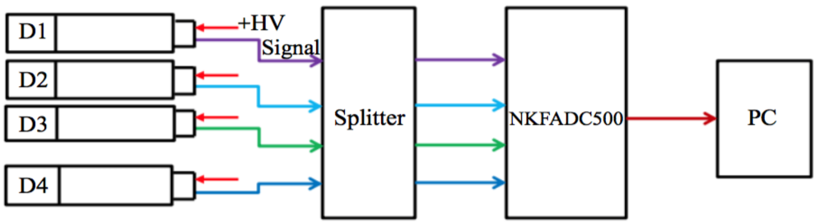

Figure 3: Schematic of an electronic illustration showing the signal from each detector.

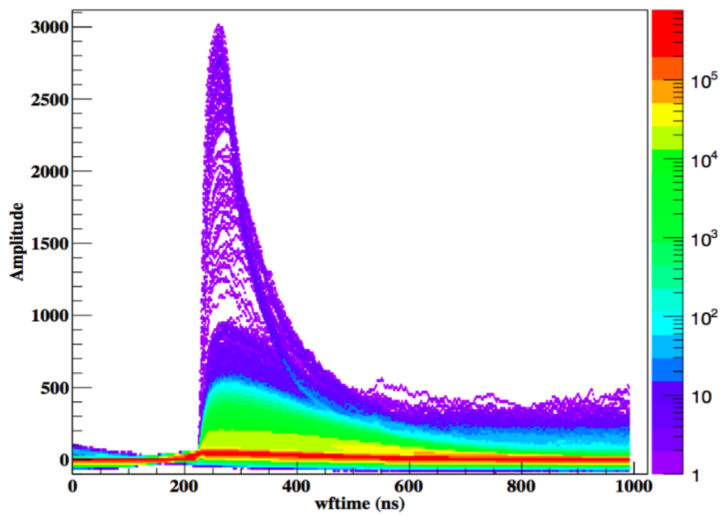

Figure 4: NaI(Tl) detector signal digitized using the NKFADC500 (500-MHz FADC).

During the measurements, the energy calibration of the spectrum was taken using standard radioactive gamma rays' sources, namely ^{60}Co source with gamma-ray energies of 1.173 MeV and 1.332 MeV and ^{137}Cs source gamma-ray energy of 0.662 MeV (Knoll 1999). Then, the three calibrated data points were fitted using a least-squared Chi-square linear fit to convert channel number to its corresponding energy value as shown in Figure 5 (a) and (b).

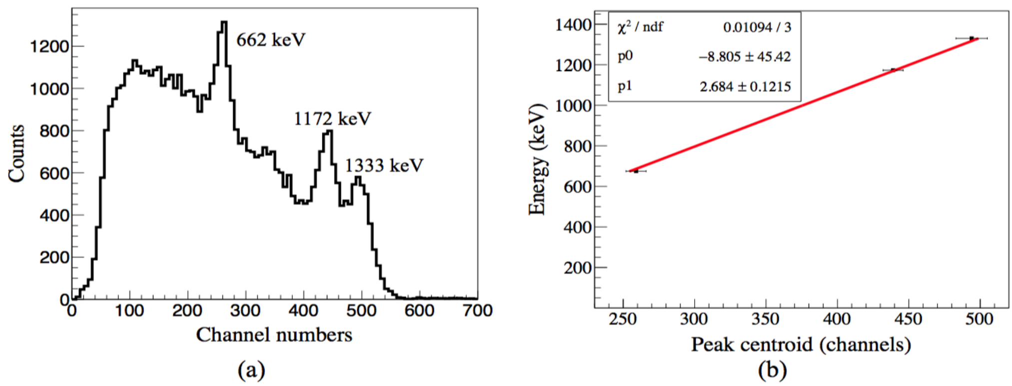

Figure 5: (a) The gamma-ray spectrum of ^{137}Cs and ^{60}Co used for energy calibrations. (b) The energy calibrations for one of the detectors used, all fittings were done using the polynomial function of order one.

The background photon energy spectrum was measured for 10 hours and was normalized with the data taking time and subtracted from the raw spectra for bremsstrahlung photon measurements. In order to take the geometric acceptance and also the energy-dependent detection efficiency into account, the Monte Carlo simulation based on the Geant4 package was performed. The simulated efficiencies were used to correct the measured bremsstrahlung photons spectra in all azimuthal angles. Furthermore, all the measured bremsstrahlung photons spectra were normalized to the number of yields taken in the same time interval by the detector D4 located at the view port.

Monte Carlo Simulations

The simulation setup to measure the angular distributions of the bremsstrahlung photons in this study followed the same procedures as the experimental setup except the photons were measured at 12 azimuthal angle including bottom part of the ECR ion source. The Monte Carlo (MC) simulation techniques based on the Geant4 package were conducted to study photon yields of each azimuthal angle. However, before performing the Geant4 simulation, based on the full geometry of the KBSI ECR ion source structure, the validity of the simulated codes software was checked. The accuracy of the response function was verified by the comparison with experimental measurements. The comparison of the measured and the simulated spectra were done using radioactive standard gamma source of ^{137}Cs as displayed in Figure 6. It is clear from Figure 6 that, there is a good agreement between the simulated and the measured spectra around the photo-peak region, but the slight deviation is observed below 200 keV. The simulated and the measured spectra show a peak at around 200 keV that is caused by Compton backscattering. It is also observed that the simulated spectra show lower counts between Compton edge and the photo-peak that might be caused by single Gaussian function for broadening.

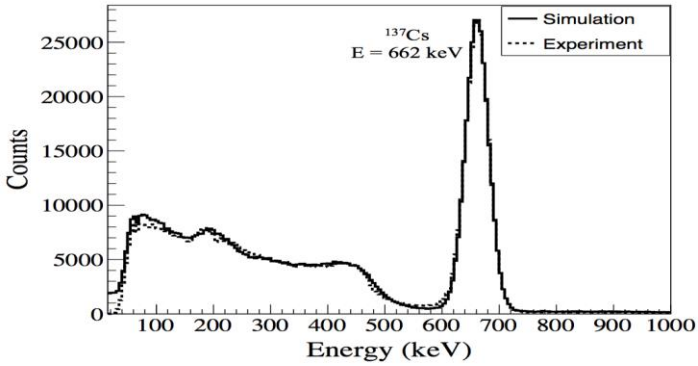

Figure 6: Comparison of the experiment and the simulation for the standard radioactive source ^{137}Cs with the gamma-ray energy 0. 662 MeV.

To perform the Monte Carlo simulation based on Geant4 package, the full geometry of the KBSI ECR ion source design was considered as shown in Figure 7. Furthermore, the internal structure of the ECR plasma is formed in the shape of a twisted triangular prism (Benitez et al. 2008, Mironov and Beijers 2009, Mironov et al. 2015), thus, the simulation was based on the triangular shape of the ECR plasma as drawn from Geant4 simulation standard model. The simulation results were obtained for the inverted triangular volume source emitting energy photons in each azimuthal angle at 1.3 MeV.

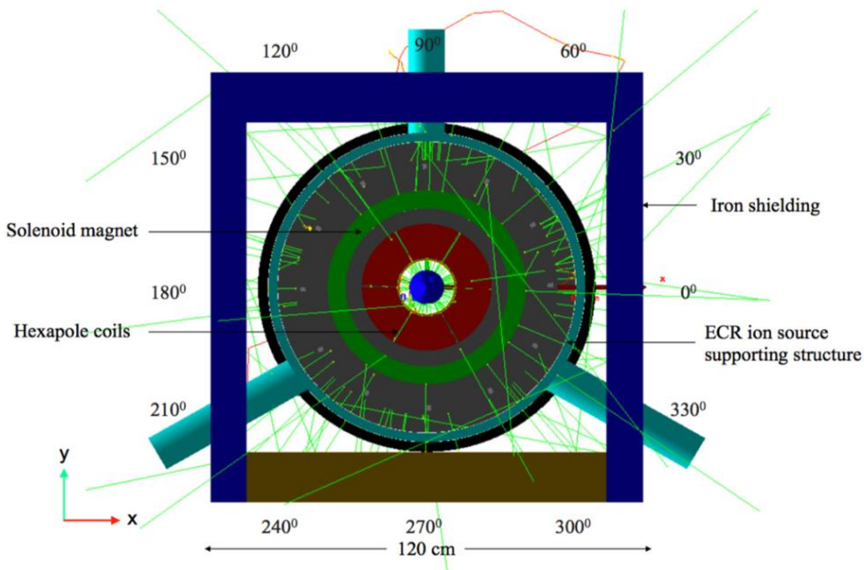

Figure 7: Schematic view of twelve azimuthal angles as simulated from the Geant4 simulation package. The schematic view also shows the real events display from the Geant4 simulation.

Results and Discussions

Experimental Data and Simulation Results

The measured and simulated energy spectra of the bremsstrahlung photons at the extraction side of the ECR ion source for different azimuthal angles were measured using NaI(TI) scintillation detector. Figure 8 (a) and (b) show measured and simulated energy spectra of the bremsstrahlung photons, respectively. The peak structures appear around 0.3 MeV in both measured and simulated spectra are most likely caused by the combination of attenuation of photons through various materials in the source as well as cumulative Compton backscattering contribution associated with low-energy bremsstrahlung photons. The photon intensity changes drastically according to the azimuthal angles. The slope in the high-energy tail from both the measured and the simulated spectra indicates the characteristics of the source of the bremsstrahlung photons. Moreover, the 150° energy spectrum (measured) shows a long tail near 2.040 MeV, while simulated spectrum at the same angle shows end point energy of 1.850 MeV, which are both beyond the maximum kinetic energy available from ECR heating. Based on the ECRIS operating parameters, the maximum kinetic energy would approximately be 1.330 MeV if the energy resolution of the NaI(TI) detector of 7% is considered.

The Compton backscattering contribution from bremsstrahlung events have a different effect on the shape of the bremsstrahlung photons energy spectra, and it is removed from the spectra by deconvolution technique. The deconvolution technique was applied to the experimental measured bremsstrahlung photons for all nine measured azimuthal angles, in the similar way the deconvolution technique was also applied to the simulation software to obtain true simulated bremsstrahlung photons. By implementing inverse matrix deconvolution technique to the continuous spectrum, the results show a more precise identification of end-point energy in the spectrum as well as removal of electronics fluctuations in the measured and the simulated spectra.

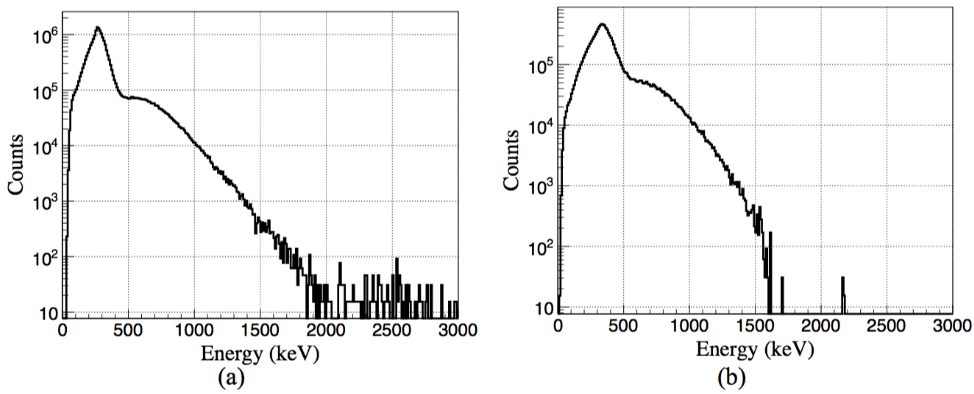

Figure 8: (a) The measured bremsstrahlung photons at an angle 150° using detector D1 (NaI(TI) scintillation detector). (b) The simulated bremsstrahlung photons at an angle 150° using NaI(TI) scintillation detector.

Figure 9 and Figure 10 indicate the measured angular distributions of the integrated photons yields after unfolding of the measured bremsstrahlung photons spectra. The photons yields were integrated into three energy regions, namely low-energy$\left(0.400 \le E_\gamma < 0.700 \text{ MeV}\right)$, mid-energy$\left(0.700 \le E_\gamma < 1.000 \text{ MeV}\right)$, and high-energy$\left(1.000 \le E_\gamma < 1.300 \text{ MeV}\right)$ using ROOT V.5.4. The starting energy point was set to be 0.4 MeV due to the fact that in a typical ECR ion source the total material thickness in the radial direction is several tens of millimetres and consists of different elements. Due to the material thickness, the lower energy part of the bremsstrahlung spectrum is largely damped as the radiation penetrates to the complicated structure. Threshold selection of 0.4 MeV is based on Geant4 simulation of the full geometry of the KBSI ECR ion source.

The number of events after the deconvolution increases in the middle and high-energy regions for all 9 integrated azimuthal angles as shown in Figure 9. The integrated photon yields are almost two orders of magnitudes different between the maximum and the minimum yields. The two maxima angles are150° and 330°, which are 180° opposite to each other. It is interesting that the integrated photon yields in the three energy regions are all in phase. The other two detectors (D2 and D3) show similar behaviour.

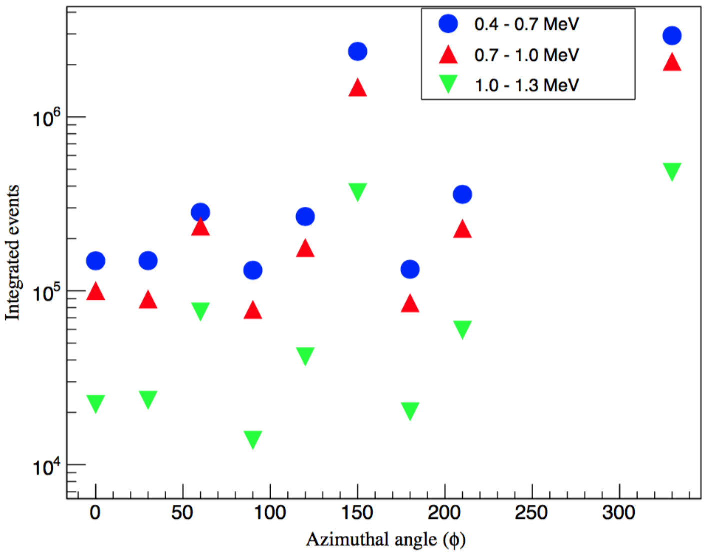

Figure 9: The angular distribution of the bremsstrahlung photons in three energy regions obtained from the measurements at the extraction side of the ECR ion source.

The ECR plasma is formed in the shape of a twisted triangular prism, due to the hexapole fields. The cross-section of the ECR plasma was an inverted triangle at the extraction side of the ECR ion source. Electrons at three corners of the triangle can easily interact with the chamber wall and produce the bremsstrahlung photons. The three corners of the plasma triangle correspond to the angles of 30°, 150° and 270°. The last angle position was not accessible due to the additional supporting structure. The corner at 150° corresponds to one of the maximum angles, while the second corner at 30° is off the local maximum point at 60°. Moreover, the high photon yields at angles 210° and 330° cannot be explained with the shape of the ECR plasma.

Figure 10 depicts the integrated photon yields regarding the twelve azimuthal angles as simulated from the Geant4 simulation based on the full geometry of the ECR ion source in three energy regions as in the experiment. The integrated photon yields reach maximum at angles 30°, 150° and 270°, corresponding to the three angles of the inverted triangle in the measurement plane. It should be noted that angle 90° is 180° opposite to maximum angle 270°. The gaps between the adjacent hexapole coils could account for photons yields observed at angles 0° and 180°. The additional thickness of the iron shielding of the ECR ion source at the top and the bottom sides reduces yields, corresponding to the angular 60°, 120°, 240° and 300°, respectively. It is interesting that the simulated photon yields at angle 150° were correlated with the measured photon yields at angle 150° at the extraction side. The maximum points appear at every 120° angle as expected, due to the inverted triangular shape of the ECR plasma. The results also show that the integrated photon yields in all three energy regions are in phase.

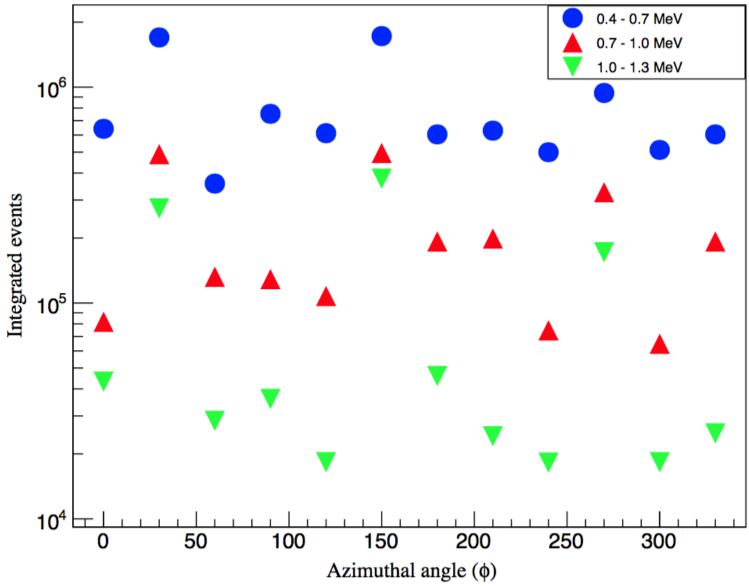

Figure 10: Angular distributions of the bremsstrahlung photons of the twelve azimuthal angles obtained from the Geant4 simulation of the inverted triangular volume source.

Figures 11 (a), (b) and (c) show summary of the results of comparison of the angular distributions of the bremsstrahlung photons at nine and twelve azimuthal angles obtained from the measurements and the Geant4 simulation, respectively, in each energy regions. The integrated photon yields are almost one order of magnitude different between the simulated and measured photon yields. Figure 11 (b) shows three corner points which are intersected, namely 0°, 150° and 210°. It was also observed that the corner at 150° was correlated in all three energy regions. It should be noted that, the correlated corner point at 150° corresponds to one of the maximum angles of the inverted triangle at the extraction side of the ECR ion source. Furthermore, from both the simulation and the measurements, the minimum integrated photon yields are observed at the high-energy region in the order of magnitude ranging between 10^4 and 10^5, whereas the maximum photon yields are observed at the low-energy region in the order of magnitude up to 10^6.

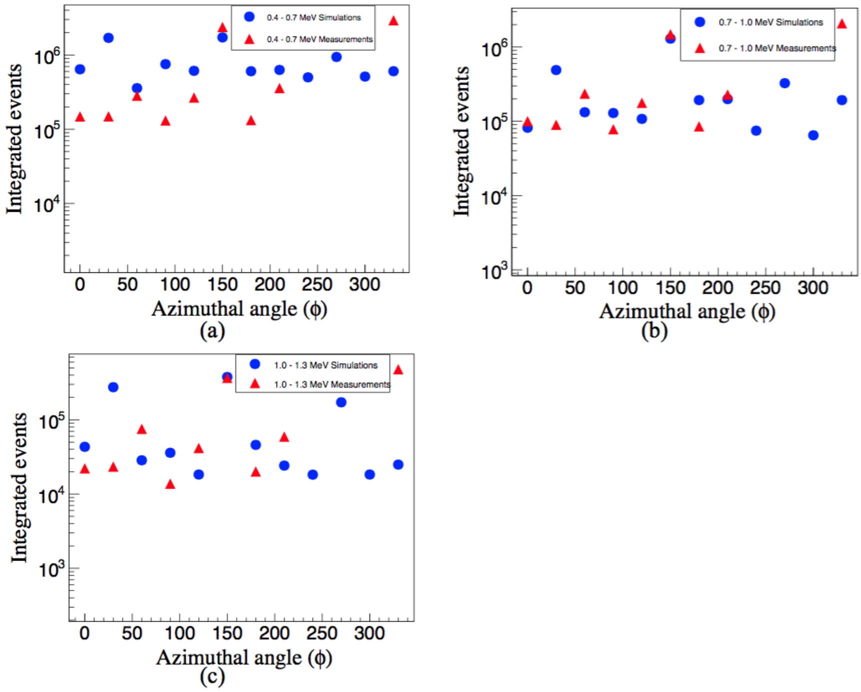

Figure 11: Comparison of the angular distributions of the bremsstrahlung photons at nine and twelve azimuthal angles obtained from the measurements and the Geant4 simulations, respectively (a) low-energy region (b) mid-energy region and (c) high-energy region.

Conclusions

For the first time, the angular distributions of the bremsstrahlung photons from the 28-GHz ECR ion source at Busan Centre of KBSI at the extraction side were measured using NaI(TI) scintillation detectors in round type configurations. Additionally, the Monte Carlo (MC) simulations based on the Geant4 package were conducted to study the angular distributions of the bremsstrahlung photons of each azimuthal angle at the extraction sides using the same detectors configurations as in the experiment. It was observed that the maximum simulated photon yields at angle 150° is a coincidence with the maximum measured photon yields at angle 150° at the extraction side which can be explained by the internal structure and shape of ECR plasma. Therefore, the maximum number of photons events observed at an angle 150° from both the measurements and simulation is due to higher numbers of unconfined electrons arriving at the chamber wall easily, and produce higher bremsstrahlung photons. The unconfined electrons are the results of imperfect magnetic confinements that cause electrons to escape from the plasma volume.

Acknowledgements

The author acknowledges the efforts put to this work by Prof. Jung K. Ahn and Dr. J.W. Lee and all other members of Hadron and Nuclear Physics Laboratory (HANUL) of the Department of Physics, Korea University. The author is also thankful to the Korea Basic Science Institute for hosting the experiments at the KBSI-PNU Laboratory. The author also gratefully acknowledges the financial support by National Research Foundation of Korea, Korea University, KBSI and the University of Dar es Salaam.

References

Benitez JY, Noland JD, Leitner D, Lyneis C, Todd DS and Verboncoeur J 2008 High energy component of X-ray spectra in

ECR ion sources. *In Proc. ECRIS'08*, Chicago, IL, USA, 77-84.

Kasthurirangan S, Agnihotri AN, Desai CA and Tribedi LC 2012 Temperature diagnostics of ECR plasma by measurement of electron bremsstrahlung. *Rev. Sci. Instrum* 83: 073111.

Kumwenda MJ, Ahn JK, Lee JW, Lugendo IJ, Kim SJ, Park JY and Won MS 2017 Angular distributions of Bremsstrahlung photons from ECR Plasma. *J. Korean Phys. Soc.* 71: 780-784.

Kumwenda MJ 2018 *Measurements of Bremsstrahlung Photons in 28 GHz Electron Cyclotron Resonance Plasma*. PhD Thesis, Korea University.

Knoll GF 1999 Radiation Detection and Measurement. 3rd ed, John Wiley & Sons, Inc.

Leitner D, Lyneis CM, Loew T, Todd DS, Virostek S and Tarvainen O 2006 Status report of the 28 GHz superconducting electron cyclotron resonance ion source VENUS. *Rev. Sci. Instr.* 77: 03A302.

Leitner D, Benitez JY, Lyneis CM, Todd DS, Ropponen T, Ropponen J, Koivisto H and Gammino S 2007 Measurement of the high energy component of the X-ray spectra in the VENUS ECR ion source. *In Proc of the 12th International Conference on Ion Sources*, Jeju, Korea, August 2007.

Lee BS, Choi S, Yoon JH, Park JY and Won MS 2012 Manufacturing of a superconducting magnet system for 28 GHz electron cyclotron resonance ion source at KBSI. *Rev. Sci. Instrum*. 83: 02A347.

Lieberman MA and Lichtenberg AJ 2005 Principles of plasma discharges and materials *processing*. 2nd ed, John Wiley & Sons.

Mironov V, Bogomolov S, Bondarchenko A, Efremov A and Loginov V 2015 Numerical model of electron cyclotron resonance ion source. *Phys. Rev. Spec. Topics- Accel. Beams* 18: 123401.

Mironov V and Beijers JPM 2009 Three-dimensional simulations of ion dynamics in the plasma of an electron cyclotron resonance ion source. *Phys. Rev. Spec. Topics – Acceler. Beams* 12(7): 073501.

Noland J, Benitez JY, Leitner D, Lyneis C and Verboncoeur J 2010 Measurement of radial and axial high energy x-ray spectra in electron cyclotron resonance ion source plasmas. *Rev. Sci. Instrum.* 81: 02A308.

Noland JD 2011 *Measurements of plasma bremsstrahlung and plasma energy density produced by electron cyclotron resonance ion source plasmas.* PhD Thesis, University of California.

Park JY, Lee BS, Choi S, Kim SJ, Ok JW, Yoon JH, Kim HG, Shin CS, Hong J, Bahng J and Won MS 2016 First results of 28 GHz superconducting electron cyclotron resonance ion source for KBSI accelerator. *Rev. Sci. Instrum*. 87: 02A717.

Park JY, Choi S, Lee BS, Yoon JH, Ok JW, Kim BC, Shin CS, Ahn JK and Won MS 2014 Superconducting magnet performance for 28 GHz electron cyclotron resonance ion source developed at the Korea Basic Science Institute. *Rev. Sci. Instrum*. 85: 02A928.

Ropponen T, Tarvainen O, Jones P, Peura P, Kalvas T, Suominen P, Koivisto H and Arje J 2009 The effect of magnetic field strength on the time evolution of high energy bremsstrahlung radiation created by an electron cyclotron resonance ion source. *Nucl. Instrum. Methods Phys. Res. Sect.* A 600: 525-533.

Zhao HY, Zhang WH, Cao Y, Zhao HW, Lu W, Zhang XZ, Zhu YH, Li XX and Xie DZ 2010 Measurements of bremsstrahlung radiation and X-ray heat load to cryostat on SECRAL. *In Proc. ECRIS'10*, Grenoble, France, paper TUPOT009: 134-136.